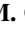




Characterisation of the neutron sources in use at STUK SSDL through a new transfer instrument with spectrometric capabilities

R. Bedogni¹, L. Russo¹, A. Calamida¹, A. I. Castro Campoy¹, M. A. Caballero-Pacheco¹, D. Dashdondog¹, E. Mafucci^{2,3}, V. Monti^{2,3}, M. Costa^{2,3}, A. Pietropaolo^{1,4,a} , J. M. Gomez-Ros^{1,5}, P. Toroi⁶, J. Huikari⁶

¹ Istituto Nazionale di Fisica Nucleare-Frascati National Laboratories, Frascati, Italy

² INFN Sezione di Torino, via Pietro Giuria 1, 10125 Turin, Italy

³ Università degli Studi di Torino, Via P. Giuria 1, 10125 Turin, Italy

⁴ Department of Fusion and Technologies for Nuclear Safety and Security, ENEA, Frascati, Italy

⁵ CIEMAT, Av. Complutense 40, 28040 Madrid, Spain

⁶ STUK-Radiation and Nuclear Safety Authority, Jokiniemenkuja 1, 01370 Vantaa, Finland

Received: 11 November 2023 / Accepted: 23 March 2024

© The Author(s) 2024

Abstract Characterising neutron sources for calibration or generic testing purposes is a complex task, as the neutron spectrum may depend, to some extent, on the construction characteristics of the source. Bonner spheres (BS) are the traditional spectrometric transfer instruments, but they are very sensitive to room scatter and required measurements are highly time consuming. The recently developed NCT-WES device, belonging to the family of the Single Moderator Neutron Spectrometers, has been proposed as a convenient alternative to BS. This work presents the results of a demonstration campaign organised at the STUK neutron metrology laboratory (Finland) in July 2023, where the spectra from two ²⁵²Cf and two ²⁴¹Am-Be sources were determined. For the ²⁴¹Am-Be sources, the results were compared to the spectra of two categories recently introduced by ISO 8529-1. Based on the results it was concluded that the “large” source category is an appropriate selection for STUK sources. The campaign also proved the operational advantages of NCT-WES as spectrometric transfer instrument.

1 Introduction

Secondary standard dosimetry laboratories (SSDL) that use radionuclide neutron sources to calibrate neutron sensitive instruments need to establish traceability to primary standard dosimetry laboratories (PSDL) for their measurements. This is preferably done by using a neutron source of the types recommended by ISO [1], which emission rate was previously determined at a PSDL with the method of the manganese sulphate bath [2]. In alternative, the SSDL source can be characterised “in situ” using a calibrated transfer instrument such as a long counter [3]. These methods focus on the source emission rate or the fluence rate and do not provide information on the energy distribution. By contrast, accurate knowledge of the energy distribution would be very valuable to SSDL as this is needed to convert the measured neutron fluence into operational quantities using energy-dependent conversion coefficients [4].

If the source is ²⁵²Cf the lack of spectral information is not a concern, as ²⁵²Cf has very large specific activity and exhibits minimal dependence of the energy distribution from the capsule type and amount of sensitive material [1]. The situation is different for (α, n) sources such as ²⁴¹Am-Be. In these sources the active material occupies up to 50 cm³ or more in volume, and a dependence of the spectrum from the capsule type and amount of material was recognised, mainly in the energy range below approximately 2 MeV [5, 6]. On this basis, in its 2021 revision of the 8529-1 Standard, ISO introduced two spectral categories in addition the ²⁴¹Am-Be spectrum already included in the 2001 version of the same standard [7]: the “small” and “large” ²⁴¹Am-Be source spectra, described in detail down to thermal energies.

The “small” source category refers to an americium activity in the order of 40 GBq and indicative size 22 mm (diameter) × 31 mm (height). The “large” source category refers to an americium activity in the order from 185 to 555 GBq and indicative size 30 mm (diameter) × 60 mm (height).

Although the spectral differences between these two categories are limited, they can have important impact when calibrating devices with prominent energy dependence, such albedo-type personal dosimeters [8, 9].

As a consequence of these considerations, prior to its use in a SSDL, an ²⁴¹Am-Be source should be characterised not only in terms of emission rate but also in terms of energy distribution.

^a e-mail: antonino.pietropaolo@enea.it (corresponding author)

Bonner spheres (BS) [10] may help filling this gap of spectral information, but their use requires significant logistic effort and is very lengthy. Also, BS are isotropic and thus very sensitive to room scatter. Of the scatter correction techniques recommended by ISO 8529-2 [11], the “shadow cones” one is certainly the quickest. However, even with this technique, the full characterisation of a calibration-grade source in an irradiation room could easily take one week of measurements, or more.

In the last decade a new class of single-moderator neutron spectrometers (SMNS) has been developed [10, 12–14]. These devices condense the functionality of BSS in a single moderator with specific geometry, embedding multiple solid-state thermal neutron detectors in previously optimized positions. SMNS are similar to BSS in terms of energy interval, operation, unfolding and performance, but they require only one exposure to determine the whole neutron spectrum. NCT-WES (neutron capture therapy wide energy spectrometer) [15] is a SMNS with sharply directional response based on a collimated cylinder. NCT-WES is nearly insensitive to the scattered field, so it is very convenient for the characterisation of neutron sources. Owing on a pair of measurements at the same distance from the source, one in “total field” and the other with shadow-cone, NCT-WES derives the full source spectrum with BSS-like performance.

With the aim of demonstrating the potentialities of NCT-WES for neutron metrology, a measurement campaign was organised at STUK SSDL (Finland) in July 2023. Four neutron sources were characterised with NCT-WES:

- Two ^{252}Cf sources with emission rate of about 10^7 s^{-1} and $3 \times 10^7 \text{ s}^{-1}$. The purpose was to confirm that the ISO-tabulated ^{252}Cf spectrum [1] well describes real Cf sources, disregarding the capsule type and amount of active material.
- Two $^{241}\text{Am-Be}$ sources with emission rate of about $2 \times 10^6 \text{ s}^{-1}$ and $2 \times 10^7 \text{ s}^{-1}$ in the same type of capsule. The purposes were to provide source-specific neutron spectra and to verify whether the new ISO spectral categories can be useful in this practical case.

2 The NCT-WES device

Although NCT-WES (See Fig. 1) is already described in Ref [15], few constructive details are repeated here to improve readability. It is a polyethylene cylinder with 36 cm diameter and 41.5 cm height. The cylindrical collimator is internally lined with 0.5 cm of borated rubber and has length 20 cm and internal diameter 11 cm. The collimator is followed by the sensitive capsule that embeds six thermal neutron detectors at different depths along the cylindrical axis of the device. To improve the directionality of the response, the sensitive capsule is protected with 0.5 cm of borated rubber in all directions except that identified by the collimator. The centres of the internal detectors are located along the cylindrical axis at different distances from the spectrometer front face, namely: 20.22 (shallowest detector in position P1), 21.52, 22.82, 24.12, 26.12 and 28.12 cm (deepest detector in position P6). The internal thermal neutron detectors are 1 cm^2 , ^6LiF -coated, windowless $p-i-n$ diodes featuring depleted layer of about $106 \mu\text{m}$. The ^6LiF coating is $30 \mu\text{m}$ thick which proved to maximise detection efficiency [16–18].

NCT-WES computational model was with MCNP 6 [19], using the ENDF/B-VIII [20] neutron cross-section libraries below 20 MeV and room-temperature cross-section tables in polyethylene, $S(\alpha, \beta)$. The signal in the internal thermal neutron sensors was simulated starting from the number of (n, t) reactions in the ^6LiF radiator. The “expected” number of pulses was then obtained

Fig. 1 Scheme of NCT-WES

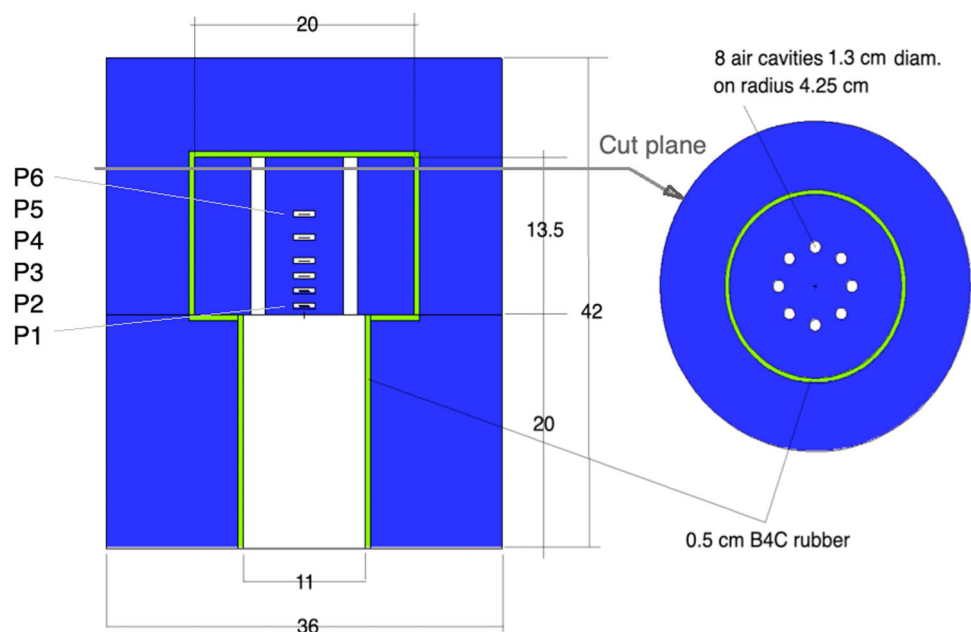


Fig. 2 Simulated Response of NCT-WES at SDD = 150 cm in terms of expected number of pulses per emitted neutron. Symbols P1 to P6 indicate the detector positions from the shallowest to the deepest

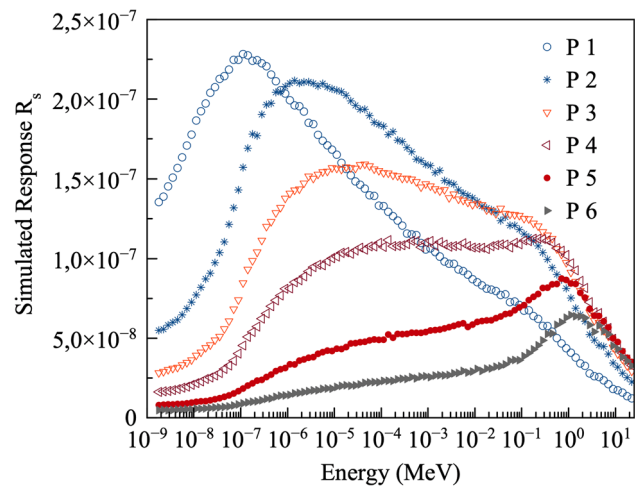
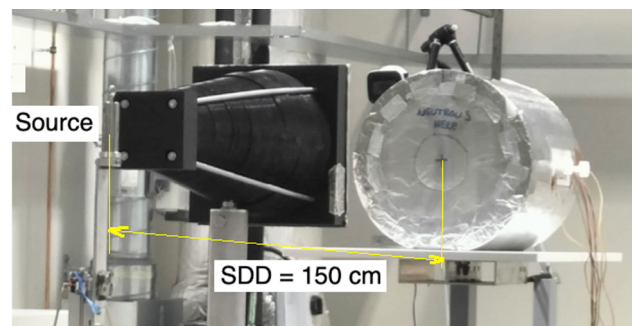


Fig. 3 The irradiation set-up with the shadow-cone in place



by multiplying this estimator by a scaling factor, previously estimated through exposure in reference neutron fields including monoenergetic neutrons [15, 18].

As described in Sect. 3, the device was exposed with its front face at 150 cm from the centre of the neutron source (Source-to-detector distance SDD = 150 cm). As this distance is comparable with the size of the spectrometer, the device is not uniformly irradiated. Therefore, as done in Ref [18], a distance-specific response matrix, $R_i = R(\text{SDD}, E)$, was derived, where “ i ” indicates the position of the internal detector (see Fig. 2) from the shallowest (P1) to the deepest (P6).

3 Irradiation facility and neutron sources

STUK’s neutron metrology room [21] has dimensions 5 m (width) \times 5 m (height) \times 16 m (length). The walls of the irradiation room are 1 m thick heavy concrete with average density of 3600 kg cm^{-3} . The increase of density is achieved by adding iron ore to concrete.

The neutron sources characteristics are given below:

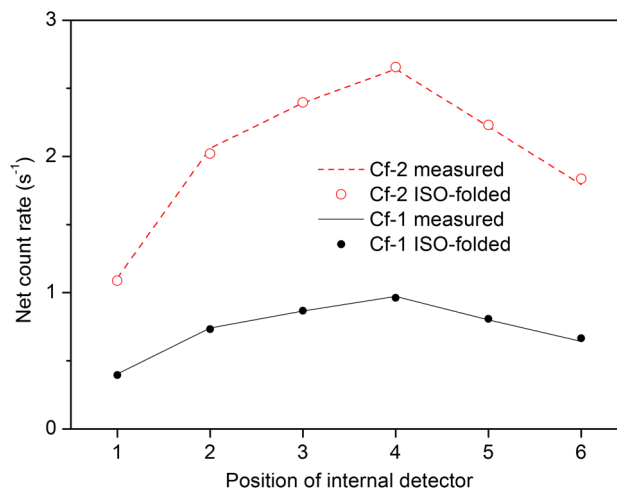
- Two ^{241}Am -Be sources with nominal emission rate $2.09 \times 10^6 \text{ s}^{-1}$ (Am-Be-1) and $1.99 \times 10^7 \text{ s}^{-1}$ (Am-Be-2) of model 4107 from Eckert & Ziegler Isotope Products, with cylindrical stainless steel double encapsulations. Approximate outer dimensions are 25.4 mm in diameter and 76.2 mm in length. The wall thickness is about 4 mm (cylinder) and 4 mm (bottom end) or 6 mm (top end). The active material is a compressed mixture of ^{241}Am oxide and beryllium..
- Two ^{252}Cf sources with nominal emission rates: $9.12 \times 10^6 \text{ s}^{-1}$ (Cf-1, date 12/7/2023) and $2.82 \times 10^7 \text{ s}^{-1}$ (Cf-2, date 12/7/2023) of model XN146 from QSA Global, Inc., with cylindrical stainless-steel encapsulations. Approximate outer dimensions are 6.1 mm in diameter and 7.2 mm (0.28 in.) in length. The wall thickness is about 1.35 mm (cylinder) and minimum 0.65 mm (ends). The Cf-252 is in the form of an oxide pressed into a pellet, a solid metal wire, or a ceramic. This capsule is further covered by a 5-mm thick aluminium cladding.

The shadow cone technique [11] was used to correct NCT-WES readings for the room scattering. The neutron source, the shadow cone and NCT-WES were set up on the calibration bench at a height of 2.5 m from the floor. The SDD was fixed to 150 cm. See also Fig. 3. The cone is made of high-density polyethylene with an aluminium and plastic support structure. Its length is 50 cm and the end diameters are 11 and 26 cm. Its small end was positioned at 15 cm from the source centre.

Table 1 Measurement times, with indication of the time spent for *total field* or *shadow-cone* measurements, and variability range for the scattered fraction s from position P1 (shallowest) to position P6 (deepest)

Source	measurement time (h, total + cone)	s from P1 to P6
Am-Be-1	42, 18 + 24	12 to 9%
Am-Be-2	21, 17 + 4	12 to 9%
Cf-1	23, 17 + 26	9 to 6%
Cf-2	7, 4 + 3	9 to 6%

Fig. 4 Experimental and ISO-folded count rates of the NCT-WES internal detectors for the sources Cf-1 and Cf-2. “ISO-folded” counts rates are obtained by folding the NCT-WES response matrix with the ISO-tabulated ^{252}Cf spectrum. Uncertainties are smaller than graphical symbols



The measurements took place from 10 to 14th July 2023. The measurement times, with indication of the time spent for *total field* or *shadow-cone* measurements, are given in Table 1. These measurement times were chosen to keep the difference “total-cone” always in the order of 1–2%, or lower, and to comply with facility access rules and working shifts. The variability range for the scattered fraction, s , is reported from position P1 (shallowest) to position P6 (deepest). s is here defined as the quotient between the count rate in the *shadow-cone* measurement and that in the *total field* measurement.

4 Results and discussion

4.1 Californium sources

The experimental count rates of the NCT-WES internal detectors for the sources Cf-1 and Cf-2 are reported in Fig. 4. In addition, the “ISO-folded” count rates are given. These are obtained by folding the NCT-WES response matrix with the ISO-tabulated ^{252}Cf spectrum. The good agreement between experimental and “ISO-folded” count rates demonstrates that the ISO-tabulated ^{252}Cf spectrum is suited to describe the studies sources (Fig. 4).

The “expected” source emission rate for the Cf-1 and Cf-2 sources was estimated starting from every single internal detector of NCT-WES. This is done as in Eqs. 1 and 2, where:

$$R_i = \int_0^\infty dE \times \varphi_{\text{Cf}}(E) \times R(150\text{cm}, E, i) \quad (1)$$

$$B_i = \frac{C_i}{R_i} \times \frac{1}{F_{90^\circ}} e^{\Sigma \times \text{SDD}} \quad (2)$$

If the assumed spectrum well represents the experimental one, all these estimations should agree within a low dispersion. This is clearly demonstrated in Fig. 5 for both Cf-1 and Cf-2 sources. By averaging these results, the best estimation of the source emission rates is given in Table 2 (B_{measured}).

4.2 Americium-Beryllium sources

The spectrum of the $^{241}\text{Am-Be}$ sources Am-Be-1 and Am-Be-2 was determined starting from the count rates presented in Fig. 6.

The data were unfolded with the FRUIT unfolding code in “special gradient mode” [22, 23]. The results are presented in Figs. 7, 8 and 9. The purpose of having three representations for the same spectra is that of better focusing on: (1) the whole energy domain, using equi-lethargy representation with log-E scale (Fig. 7); (2) the high-energy domain, using a linear energy scale (Fig. 8); (3)

Fig. 5 Estimation of the source emission rate for the Cf-1 and Cf-2 sources

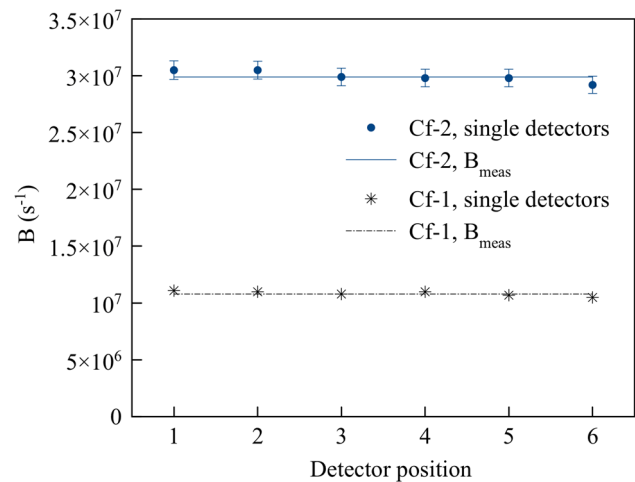
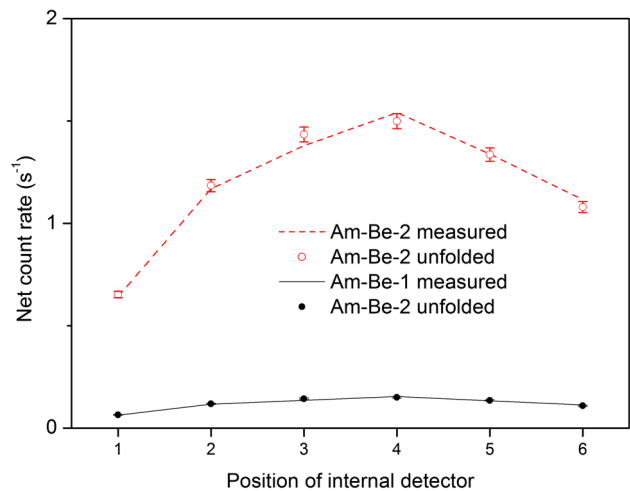


Table 2 Source emission rate as derived from the manufacturer data (B_{nominal}) or measured by NCT-WES (B_{measured})

Source	B_{nominal} (s ⁻¹) 12/7/2023	B_{measured} (s ⁻¹) 12/7/2023
Cf-1	9.12×10^6	$(1.08 \pm 0.03) \times 10^7$
Cf-2	2.82×10^7	$(2.98 \pm 0.08) \times 10^7$
Am-Be-1	2.09×10^6	$(1.98 \pm 0.05) \times 10^6$
Am-Be-2	1.99×10^7	$(1.92 \pm 0.05) \times 10^7$

Fig. 6 Experimental and “unfolded” count rates of the NCT-WES internal detectors for the sources Am-Be-1 and Am-Be-2. Uncertainties are around ±2.5%



the low-energy domain, using log–log scale (Fig. 9). For every source, two unfolding sessions were performed by using both ISO spectral categories “small source” and “large source” as “guess” spectra. The results are indistinguishable and condensed into a single solution called “STUK Am-Be-1” or “STUK-Am-Be-2”. As a standard feature of FRUIT, the bin-per-bin uncertainty superimposed on the unfolded spectrum is derived by propagating input uncertainties (BSS counts and response matrix) through the unfolding process. Together with the unfolded solution, three other spectra are reported for comparison purposes: the two spectral categories “small” and “large” from ISO 8529-1, and the “old” ²⁴¹Am-Be spectrum from the 2001 version [7] of the same Standard. Figures 7, 8 and 9 show that both Am-Be-1 and Am-Be-2 spectra are closer to the “large” source category than to the “small” or ISO 2001 spectra. This is reasonable, as the dimensions of the sources used to derive the ISO “large” source category (diameter 30 mm x height 60 mm) [5, 6] are similar to those of the 4107 capsule (diameter 25.4 mm x height 76.2 mm), used in this work.

As far as the source emission rate is concerned, the “measured” value in Table 2 was obtained using Eq. 2. In absence of source-specific values for the 90° anisotropy factor F_{90° , values from ISO [1] for sources of similar emission rate were taken. These are 1.027 ± 0.001 and 1.042 ± 0.002 for Am-Be-1 and Am-Be-2, respectively.

Fig. 7 Spectra of Am-Be-1, Am-Be-2, “small” source, “large source” and ISO-2001 in equi-lethargy representation with log-E scale

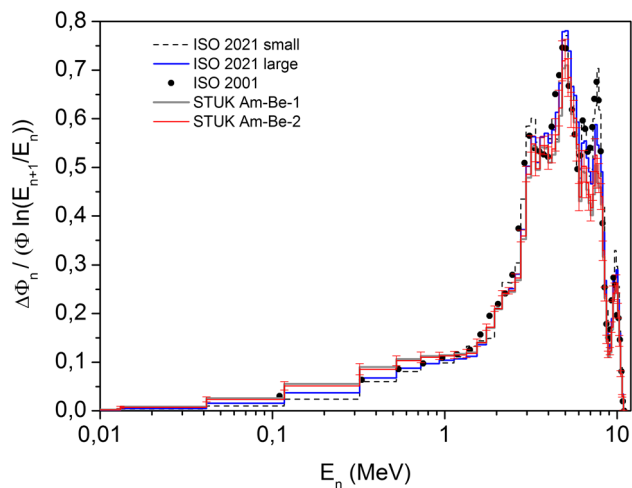


Fig. 8 Spectra of Am-Be-1, Am-Be-2, “small” source, “large source” and ISO-2001 in equi-lethargy representation and emphasising the high-energy domain through a linear energy scale

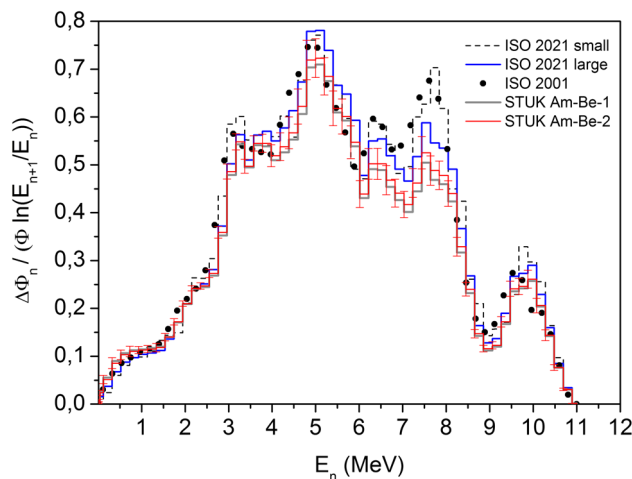
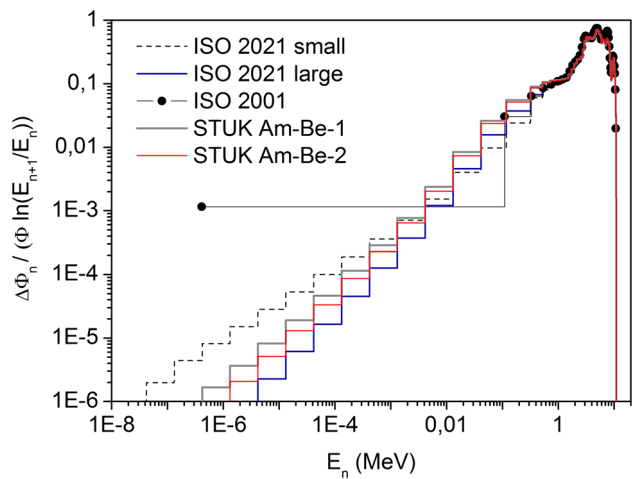


Fig. 9 Spectra of Am-Be-1, Am-Be-2, “small” source, “large source” and ISO-2001 in equi-lethargy representation and emphasising the low-energy domain through log-log scales



4.3 Measurement time and scattered radiation

Besides the spectrometric results presented in Sects. 4.1 and 4.2, it is important mentioning that the complete spectrum of a source was determined in about one day of measurements. With BS this time would be a factor of 4–5 larger, as every sphere would need a double exposure with and without shadow-cone.

In addition, as shown in Table 1, the scattering contribution to the NCT-WES internal detector readings, i.e. cone/total field measurement, was at most 12%. This is due to the collimating aperture and to the external polyethylene and borated rubber

shielding. For Bonner Spheres at similar distance this ratio would easily increase to >40% [24], thus confirming the reduced response of NCT-WES to room scatter.

5 Conclusions

By means of a dedicated testing campaign at the STUK neutron metrology lab, the NCT-WES instrument was tested as a spectrometric transfer instrument. The spectra and emission rates of two ^{252}Cf and two $^{241}\text{Am-Be}$ sources were determined, based on the shadow-cone technique, with uncertainty lower than $\pm 3\%$. For the $^{241}\text{Am-Be}$ sources, the results are compared to the spectral categories recently introduced by ISO 8529-1, finding that the “large” source category is the most suited to represent these sources. Owing to the collimating aperture and to the polyethylene and borated rubber shielding, NCT-WES’s response to room-scattered radiation was very low. The whole campaign took less than five days. These characteristics proved the operational advantages of NCT-WES as spectrometric transfer instrument.

Acknowledgements The research presented in this paper was partially financed by the INFN project ENTER_BNCT (Commissione Scientifica Nazionale CSN5 of INFN, Italy), the Spanish project NDOSCOR (PID2021-128346NB-C21, MICINN, Spain, cofounded with FEDER) and by STUK.

Funding Open access funding provided by Ente per le Nuove Tecnologie, l’Energia e l’Ambiente within the CRUI-CARE Agreement.

Data Availability Statement The data sets generated during and/or analysed during the current study are available from the corresponding author on reasonable request. The manuscript has associated data in a data repository.

Open Access This article is licensed under a Creative Commons Attribution 4.0 International License, which permits use, sharing, adaptation, distribution and reproduction in any medium or format, as long as you give appropriate credit to the original author(s) and the source, provide a link to the Creative Commons licence, and indicate if changes were made. The images or other third party material in this article are included in the article’s Creative Commons licence, unless indicated otherwise in a credit line to the material. If material is not included in the article’s Creative Commons licence and your intended use is not permitted by statutory regulation or exceeds the permitted use, you will need to obtain permission directly from the copyright holder. To view a copy of this licence, visit <http://creativecommons.org/licenses/by/4.0/>.

References

1. ISO, International standardization organization, neutron reference radiation fields—Part 1: characteristics and methods of production. ISO 8529-1:2021 (2021)
2. N. Roberts et al., *Metrologia* **58**(1A), 06025 (2021)
3. J. De Pangher, L.L. Nichols. A precision long counter for measuring fast neutron flux density, Pacific Northwest laboratory report BNWL-260, (1966)
4. ISO, International standardization organization, Neutron reference radiation fields—Part 3: Calibration of area and personal dosimeters and determination of their response as a function of neutron energy and angle of incidence. ISO 8529-3:2023 (2023)
5. D. Thomas et al., *Rad. Prot. Dosim.* **180**(1–4), 21 (2018)
6. R. Bedogni et al., *Nucl. Instrum. Meth. A* **763**, 547 (2014)
7. International standard ISO 8529. Reference neutron radiations—Part 1: characteristics and methods of production. International standard ISO 8529-1 (2001)
8. A. Pola et al., *Nucl. Instrum. Meth. A* **927**, 371 (2019)
9. J.M. Gomez-Ros, *Rad. Meas.* **161**, 106908 (2023)
10. A. Pietropaolo et al., *Phys. Rep.* **875**, 1 (2020)
11. ISO, International standardization organization, Neutron reference radiation fields—Part 2: calibration fundamentals of radiation protection devices related to the basic quantities characterizing the radiation field. ISO 8529-2:2000 (2000)
12. R. Bedogni et al., *Nucl. Instrum. Methods A* **782**, 35 (2015)
13. R. Bedogni et al., *Nucl. Instrum. Methods A* **927**, 151 (2019)
14. R. Bedogni et al., *Europhys. Lett.* **127**, 12002 (2019)
15. R. Bedogni et al., *Europhys. Lett.* **134**, 42001 (2021)
16. R. Bedogni et al., *Nucl. Instrum. Methods A* **780**, 51 (2015)
17. Bedogni et al., *Nucl. Instrum. Meth. A* **1018**, 165855 (2021)
18. Bedogni et al., *Eur. Phys. J. Plus* **138**, 270 (2023)
19. C. J. Werner (Ed.), MCNP users’ manual code version 6.2, Report LA-UR-17-29981, Los Alamos national laboratory, USA, (2017)
20. D.A. Brown et al., *Nucl. Data Sheets* **148**, 1 (2018)
21. J. Huikari et al., *Radiat. Prot. Dosim.* **180**(1–4), 66 (2018)
22. R. Bedogni et al., *Nucl. Instr. Meth. A* **580**, 1301 (2007)
23. K. Amgarou et al., *Nucl. Inst. Meth. A* **654**, 399 (2011)
24. IAEA, Establishing neutron calibrations at SSDL using ISO 8529